

Aqueous electrodeposition of iron group–vanadium binary alloys

B.Y. Yoo, M. Schwartz, K. Nobe^{*,1}

Department of Chemical Engineering, University of California, Los Angeles, CA 90095-1592, USA

Received 12 July 2004; received in revised form 10 January 2005; accepted 30 January 2005

Available online 7 April 2005

Abstract

Electrodeposition of binary iron group (IG)–vanadium (V) alloys from aqueous citrate solutions was investigated. Addition of $\text{NH}_3(\text{aq})$ and increasing solution pH resulted in increased deposit V content, but non-metallic deposits were obtained at solution $\text{pH} > 7$. Increasing current density resulted in an almost linear decrease in V content and a sharp increase in hydrogen evolution (decreased current efficiency). In general, the amount of V deposited with the IG metal increased as follows: $\text{Ni} < \text{Fe} \ll \text{Co}$. XRD spectra indicated that preferred orientations from 25 °C solutions were not displaced by elevated temperature deposits. Changes in orientation may contribute to the deposit magnetic properties; e.g., Co–V deposits with (1 0 0) planes exhibit harder magnetization than deposits with (0 0 2) planes.

© 2005 Elsevier Ltd. All rights reserved.

Keywords: Iron-group; Vanadium; Magnetic alloys

1. Introduction

Iron group alloys have generated considerable interest for a number of years due to their magnetic properties. Brenner [1] in his seminal treatise on the electrodeposition of alloys reviewed the literature of the iron group alloys up to the early 1960s. Srimathi et al. [2] provided a comprehensive review of magnetic iron group alloy electrodeposits up to 1980. Since that time there have been numerous papers on the electrodeposition of iron group alloys because of their importance in the microelectronics industry, particularly in computer technology. Special emphasis had been directed to Permalloy (80Ni20Fe) because of its attractive soft magnetic properties for computer memory applications [3–5].

One unusual phenomenon encountered in the electrodeposition of Permalloy and other iron group alloys is the so-called anomalous co-deposition. Brenner discusses this phenomenon in which the less noble metal co-deposits at a faster rate than the more noble metal [1]. A more general representation is that the metal with the faster individual elec-

trodeposition rate co-deposits at a much slower rate than the other metal. Since Brenner, there has been extensive work on anomalous co-deposition because it is crucial to take this phenomenon into account in Permalloy's manufacturing process [6]. For example, Talbot and co-workers have investigated co-deposition of the iron group binary alloys [7–9]. Dahms and Croll [10] had earlier proposed an explanation for anomalous co-deposition of Ni–Fe alloys in which adsorbed ferrous hydroxide species retard the deposition of Ni. Hessemer and Tobias [11] pointed out the importance of IG hydroxide ions in anomalous co-deposition. Additional models involving IG hydroxide ions have also been proposed by Talbot and co-workers [12,13] and Matlosz [14]. In addition to the current interest in iron group alloys for their magnetic properties, Invar (64Fe36Ni) and Super Invar (64Fe31Ni5Co) are important for their low coefficient of thermal expansion [15,16].

There has been considerable effort directed to develop alloys with soft magnetic properties superior to Permalloy due to rapid advances in areal densities of computer hard disks. Liao [17,18] has reported that 90Co10Fe electrodeposits had twice the magnetic saturation of Permalloy, low coercivity and high magnetic permeability. However, Co–Fe alloys have low corrosion resistance and electrical resistivity; deposits are too brittle for fabrication of suitable

* Corresponding author. Tel.: +1 310 8252447; fax: +1 310 8253458.

E-mail address: nobe@seas.ucla.edu (K. Nobe).

¹ ISE member.

geometrical forms. There has been much work directed to overcome shortcomings of the soft magnetic properties of 90Co10Fe by introducing a third element, such as B, Cu and V [19–21]. Vanadium, like W, Mo and the rare earth metals, has not been electrodeposited from aqueous media. However, several workers have successfully alloyed iron group metals with W and Mo by electrodeposition from aqueous baths (see refs in [21c]). Bulk Permendur (50Fe50Co), 2V-Permendur (49Fe49Co2V) and Supermendur (purified 49Fe49Co2V) have excellent soft magnetic properties but have not had extensive commercial applications due to expensive processing costs. Because of the current interest in magnetic thin films for microelectromechanical systems (MEMS) and nanoelectromechanical systems (NEMS) applications, renewed electrodeposition activity in this group of soft magnetic ternary alloys, which are characterized by high magnetic saturation, permeability, Curie temperatures and low coercivity, seems justified. Electrodeposition has advantages over other deposition technologies; these include cost effectiveness, ease of fabrication and control.

In their review of the magnetic properties of Fe–Co alloys, Chin and Wernick [22] indicated that adding Co to Fe increases B_s and reported that a B_s of 2.45 T had been obtained for 65Fe35Co; this is the highest magnetic saturation (B_s) that had been reported, thus far, in the literature. This B_s value has also been given for Permendur (50Fe50Co) in Chen's table 6.6 [23]. In addition to the reviews listed in [21c] (e.g. Refs. [13–17]), other literature reviews of work on vanadium alloys include Refs. [24,25]. Magnetic properties for Permendur, 2V-Permendur and Supermendur reported in the references cited are summarized below:

	Permendur	2 V-Permendur	Supermendur
Elect. resistivity ($\mu\Omega$ cm)	7	25	25
Magnetic saturation, B_s (T)	2.45	2.40	2.40
Remanence, B_r (T)	1.40	1.50	2.22
Maximum permeability, μ_m	5000	4000–8000	92500
Coercivity, H_c , (Oe)	2	5	0.2

The present paper focuses on the electrodeposition of IG–V binary alloys; a subsequent paper will provide experimental results of the investigation on the electrodeposition of ternary Co–Fe–V alloys.

2. Experimental

Co–V, Fe–V and Ni–V alloys were electrodeposited from citrate baths, compositions of which are given in Table 1, unless noted otherwise. Ammonium chloride was added as a conducting salt, and also to increase the concentration of NH_4^+ ions in the solution. Vanadyl sulfate (VOSO_4) was se-

Table 1
Bath Composition for Electrodeposition of Co–V, Fe–V and Ni–V

Reagent	Co–V bath (M)	Fe–V bath (M)	Ni–V bath (M)
Cobalt chloride	0.3	0	0
Ferrous chloride	0	0.15	0
Nickel chloride	0	0	0.3
Vanadyl sulfate	0.17	0.32	0.17
Ammonium chloride	1.1	1.1	1.1
Ammonium citrate	0.34	0.34	0.34

lected because of its higher solubility in water and lower oxidation state compared to other soluble vanadium salts, such as ammonium vanadate. Cobaltous, ferrous and nickelous chlorides were chosen as the iron group metal salts with the bath pH varied from 5.5 to 7.0. To prepare stable baths, the mixing sequence of the chemicals is very important to avoid formation of precipitates.

The mixing sequence is as follows: Initially, cobalt, iron or nickel salt was dissolved in deionized water and mixed with ammonium chloride and the complexer, ammonium citrate. Then, the solution pH was increased up to ~ 8 by the addition of $\text{NH}_3(\text{aq.})$ (74 mL/L from a 14.8N stock solution). With the addition of the vanadium salt, solution pH decreased to around 6.5. Final pH was adjusted by addition of either HCl or KOH (solution volume was 100 mL).

The films were electrodeposited by varying current density from 1 to 50 mA/cm². Direct current was supplied by a PAR potentiostat (model 273). Brass panels (6 cm²) served as cathodes; anodes were sheets of the appropriate iron group metals. Electrodeposition was carried out at room temperature, unless otherwise noted, and the solution was not agitated during electrodeposition.

The brass panels were first cleaned with ALCONOX, followed by dipping in a 5 vol.% HCl solution to remove organic impurities and the incipient surface oxide film. After cleaning the surface, the brass substrate was dried, weighed (before and after plating for CE calculations), then activated by immersion in 20 vol.% HCl for 1 min.

After inspection with an optical microscope (600 \times), the deposits were dissolved in nitric acid. The composition of the electrodeposits was determined by atomic adsorption spectrophotometry (AA) (Perkin-Elmer, model 280) and energy dispersive spectroscopy (EDS). Microstructure was analyzed with X-ray diffraction (XRD) and surface morphology with scanning electron microscopy (SEM). Magnetic properties were measured using a vibrating sample magnetometer (VSM, ADE Tech, Model 1660).

3. Results and discussion

3.1. Co–V electrodeposits

Fig. 1 shows EDS spectra of Co–V deposits obtained from solution compositions (Table 1) and deposition conditions

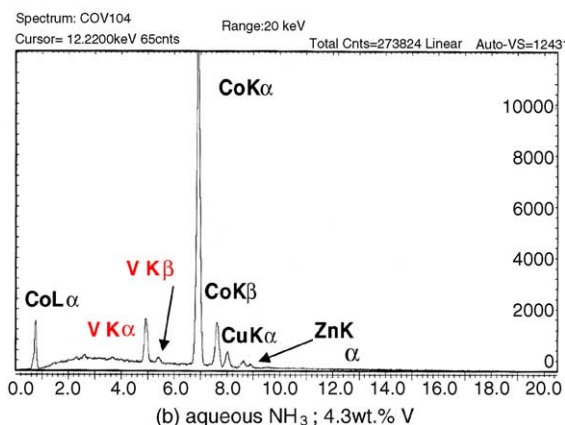
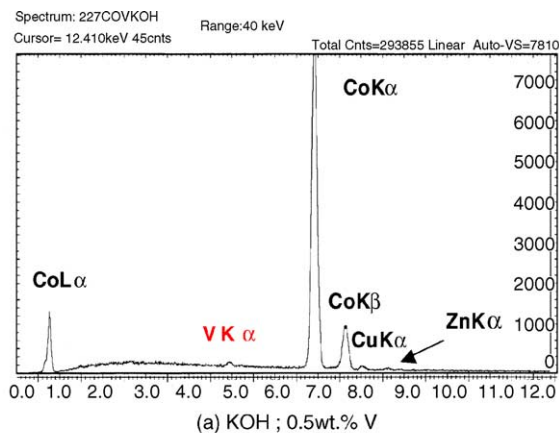


Fig. 1. EDS analysis of Co–V alloys electrodeposited with solution pH adjusted by KOH (a) or NH_3 (b); pH 6.0, CD: 5 mA/cm².

with and without addition of NH_3 (aq.). Solutions containing NH_3 (Fig. 1b) resulted in deposit V content ~ 4.3 wt.%, whereas those devoid of NH_3 (Fig. 1a) resulted in deposits with very low V content (0.5 wt.%). The presence of NH_3 (aq.) appears to function concomitantly with citrate as complexing agent. There seems to be an optimum NH_3 concentration, above which the deposit V content is increased but results in non-metallic deposits.

Doubling the vanadyl sulfate (VOSO_4) concentration from 0.1 to 0.2 M ($\text{Co} = 0.3$ M) resulted in a slight increase in deposit V content (Table 2). The cathode current efficiency (CE) reached a maximum (71%) at 0.17 M VOSO_4 concentration. In subsequent studies, the VOSO_4 and CoCl_2 concentrations were maintained at 0.17 and 0.3 M, respectively.

Table 2
Effect of VO^{2+} concentration on the deposit composition and current efficiency of Co–V electrodeposits

VO^{2+} (M)	Co (wt.%)	V (wt.%)	CE (%)
0.10	95.4	4.6	32
0.135	96.7	3.3	44
0.17	95.0	4.3	71
0.20	94.8	5.2	59

CD: 5 mA/cm², pH 6.0.

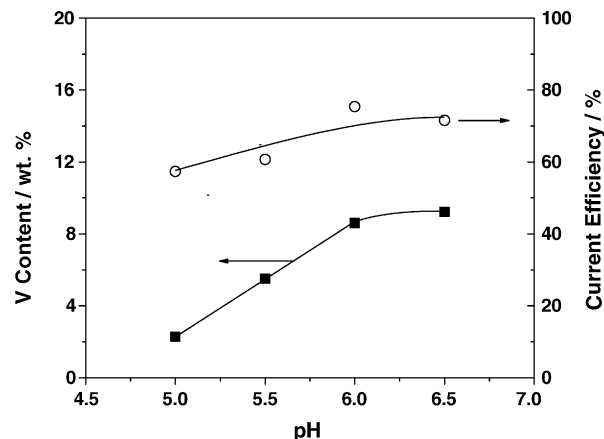


Fig. 2. Effect of pH on the composition and current efficiency of Co–V electrodeposits; CD: 3 mA/cm².

Increasing the solution pH from 5.0 to 6.0 (Fig. 2) resulted in a linear increase in deposit V content from 2.3 to 8.6 wt.%; increasing solution pH to 6.5 further increased V content slightly (9.2 wt.%). The CE increased from 57 to 72%. With solution pH > 6.5, dull, dark deposits were obtained, indicating the presence of oxides and/or hydroxides. Subsequent deposits were made from solutions maintained at pH 6.0. In previous studies [21c], no V was detected in Co deposits from slightly differing solution composition at pH 5.5 and only ~ 1 wt.% V in deposits from pH 7.0 solutions. This difference with present results may be attributed to the inhibiting presence of borate and the uncontrolled additions of NH_3 (aq.) to maintain pH. Further, solution preparation (sequence of mixing) differed from the present procedure.

Fig. 3 shows the influence of applied current densities (CD) on the deposit Co and V contents. Between 1 and 10 mA cm⁻² there is a sharp increase in deposit Co content with a corresponding decrease in deposit V content. These ‘trends’ are reduced with CDs > 10 mA cm⁻²; at 50 mA cm⁻² the deposit composition is 98.8 wt.% Co and 1.2 wt.% V as

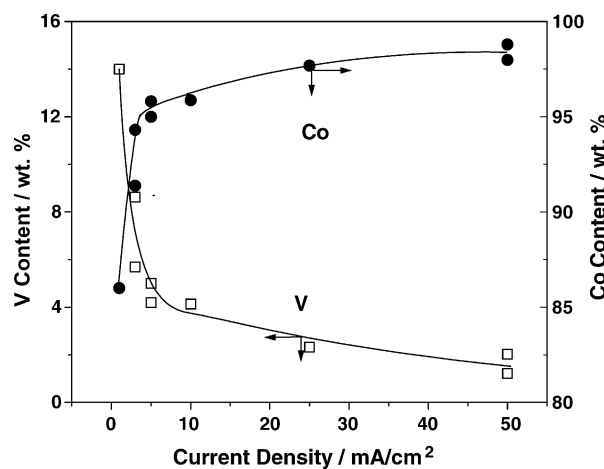


Fig. 3. Composition of Co–V electrodeposits obtained at various current densities; pH 6.0, deposit thickness = 1.2 μm .

Table 3

Deposit composition and magnetic properties of Co–V electrodeposits obtained at various current densities

CD (mA/cm ²)	Co–V					Co
	Co (wt%)	V (wt.%)	CE (%)	H_c (Oe)	B_s (T)	H_c (Oe)
1	86.0	14.0	77	142	1.41	
3	91.4	8.6	76	118	1.43	42
5	95.7	4.3	71	86	1.52	53
10	95.9	4.1	64	62	1.55	58
25	97.7	2.3	34	13	1.53	–
50	98.8	1.2	33	10	1.51	43

pH 6.0; deposit thickness = 1.2 μm .

indicated in Table 3. Deposits at $CD < 10 \text{ mA cm}^{-2}$ are accompanied with low hydrogen evolution which increases with increasing CDs. The magnetic saturation (B_s) increased and the coercivity (H_c) decreased with decreasing deposit V contents.

Co–V electrodeposits show a preferred HCP (002) orientation, indicating a basal plane parallel to the deposit surface (Fig. 4a and b). The peak intensity decreases with increasing deposit V content, a result of decreasing applied CDs. Deposits (8.6 wt.% V) obtained at 3 mA cm^{-2} , show a preferred HCP (100) orientation indicating a basal plane perpendicular to the surface (Fig. 4c). This change in preferred orientation is evidently due to the increased deposit V content, possibly contributing to the deposit magnetic properties. The grain size (GS) of electrodeposited Co–V with 1.2 and 4.3 wt.% V did not vary significantly: 12–14 nm in the (002) plane and 16 nm in the (110) plane. Co–V deposited

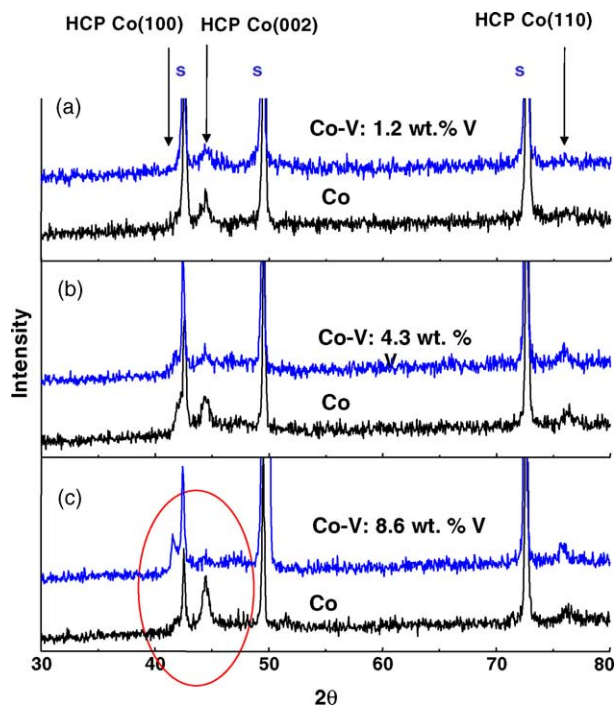


Fig. 4. XRD analysis of Co and Co–V electrodeposits at different current densities; pH 6.0: (a) $CD = 50 \text{ mA cm}^{-2}$; (b) $CD = 5 \text{ mA cm}^{-2}$; (c) $CD = 3 \text{ mA cm}^{-2}$.

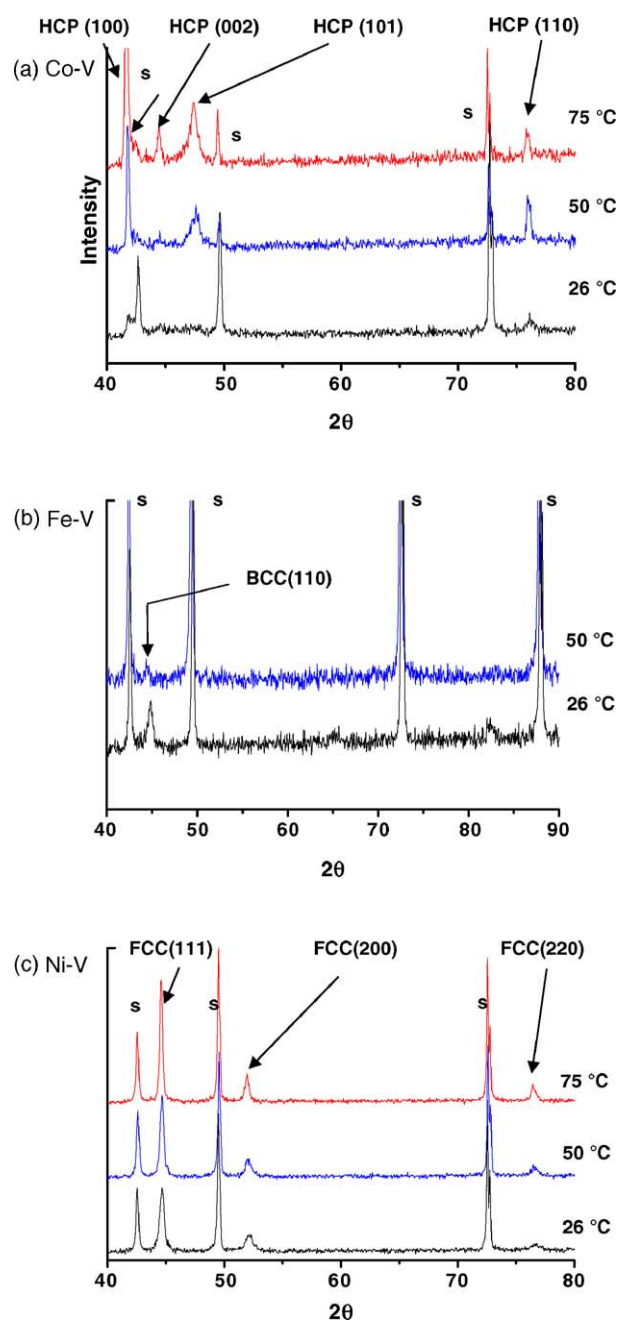


Fig. 5. XRD results of binary iron group–V alloy deposits at different temperatures; pH 6.0; $CD = 3 \text{ mA cm}^{-2}$.

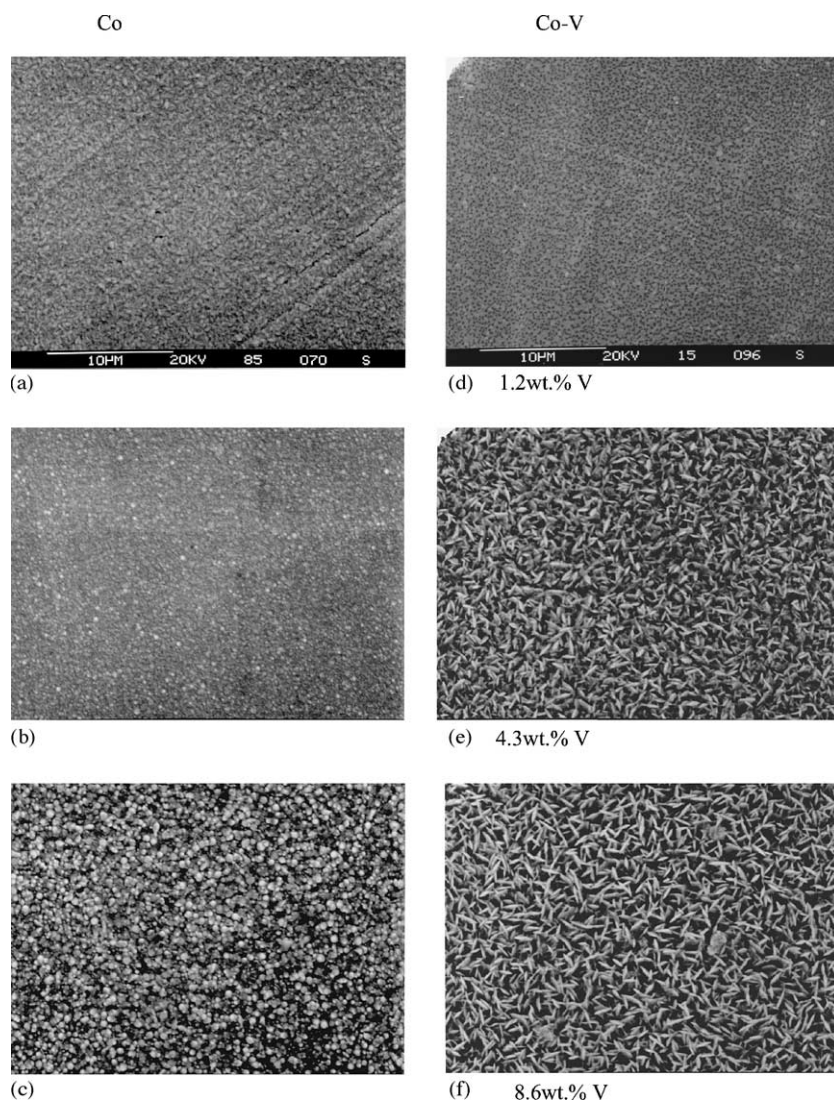


Fig. 6. SEM of Co (a)–(c) and Co–V (d)–(f) electrodeposits at pH 6.0 and various CDs; (a) and (d): 50 mA/cm^2 , (b) and (e): 5 mA/cm^2 , (c) and (f): 3 mA/cm^2 .

at lower CD (3 mA cm^{-2}) exhibited GS = 41 nm (1 0 0) plane and 14 nm (1 1 0) plane. Co electrodeposits in the same CD range also show a preferred HCP (0 0 2) orientation; no changed orientation at the lower CDs was observed, however.

The structure of Co–V deposits varies with deposition from elevated solution temperature (CD = 3 mA cm^{-2} , pH 6.0), resulting in V contents $>6 \text{ wt}\%$ (Fig. 5a). XRD spectra indicate HCP (1 0 0) and (1 1 0) planes, and HCP (1 0 0), (1 1 0), (0 0 2) and (1 0 1) planes from solutions at 26 and $50\text{--}75^\circ\text{C}$, respectively, with preferred (1 0 0) orientation. The peak intensities and broadening increased with increasing solution temperature, indicating increased GS.

The differences in surface morphology of electrodeposited Co and Co–V at various CDs is shown in Fig. 6. The surfaces of both Co and Co–V are quite similar, smooth with uniform distribution of fine nodules when deposited at the higher CD (50 mA cm^{-2}). Decreasing CD to 5 and 3 mA cm^{-2} resulted in changes in Co–V alloy surfaces to granular, acicular

(needle-like), dendritic structure with increasing porosity; Co deposits, however, became increasingly nodular. The changing morphology of Co–V alloys is apparently a result of increased V incorporated into the Co matrix.

Armyanov [26] showed that generally the easy direction of magnetization is parallel in the basal c-axis plane for HCP (0 0 2) Co deposits. Therefore, Co deposits with preferred (0 0 2) orientation exhibit harder magnetization (higher coercivities) than HCP (1 0 0) Co–V deposits which are perpendicular to the basal plane because of crystal anisotropy [26]. Fig. 4 shows that with increasing deposit V content, the (1 0 0) plane in the Co–V deposits becomes the preferred orientation, possibly accounting for the reversal in coercivities shown in Fig. 7; i.e., Co–V electrodeposits with (1 0 0) planes exhibit harder magnetization behavior than Co electrodeposits; $H_c(\text{Co–V}) \sim 2.8 X > H_c(\text{Co})$. This change indicates magnetization anisotropy might be stronger than crystal anisotropy in Co–V electrodeposits. Co electrodeposits at 3 mA cm^{-2} have a smoother, slightly nodular surface, whereas Co–V elec-

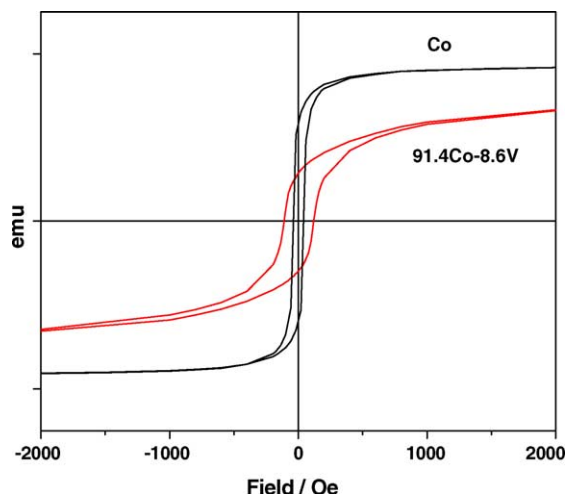


Fig. 7. Magnetic hysteresis curves (M) of Co and Co-V electrodeposits; pH 6.0, CD: 3 mA/cm², deposit thickness = 1.2 μ m.

trodeposits have an acicular, needle-like morphology (Fig. 6) which results in the shape anisotropy induced by asymmetry; i.e., it is easier to magnetize the deposit along the long axis than the short axis of magnetic films perpendicular to the surface. As indicated in Fig. 7, magnetic saturation of Co-V deposits with increased V content require stronger external fields. Table 4 shows magnetic saturation of Co deposits (1.75 T) to be ~ 1.23 X greater than Co-V (1.43 T). The coercivity of the Co-V electrodeposit (~ 118 Oe) is ~ 3 X greater than the Co deposit (~ 42 Oe). The squareness, B_r/B_s , of the hysteresis loops were Co = 0.41 and Co-V = 0.34, respectively.

The coercivity of Co-V deposits appears to be a function of the deposit V content. It decreases with decreased deposit V content, which in turn, is related to increased CD (Table 3). Thus, deposits ~ 14 wt.% V (CD = 1 mA cm⁻²) exhibit a coercivity of ~ 142 Oe, whereas deposits ~ 1.2 wt.% V (CD = 50 mA cm⁻²) exhibit a coercivity ~ 10 Oe. Increased V content increases deposit coercivity probably because vanadium being non-magnetic acts to obstruct magnetic wall movement [23]. Magnetic saturation, B_s , increases with increased CD, from 1.41 to 1.51 T, also as a result of the concomitantly lowered deposit V and increased Co contents (Table 3). Coercivities of cobalt electrodeposited in this CD range did not vary substantially.

Table 4
Effect of vanadium on the magnetic properties of iron group metals

Material	Composition	H_c (Oe)	B_s (T)
Co	100Co	42	1.75
Co-V	91.4Co-8.6V	118	1.43
Fe	100Fe	94	2.10
Fe-V	98.5Fe-1.5V	27	2.05
Ni	100Ni	89	0.60
Ni-V	99.3Ni-0.7V	102	-

CD: 3 mA/cm²; pH 6.0; deposit thickness = 1.2 μ m.

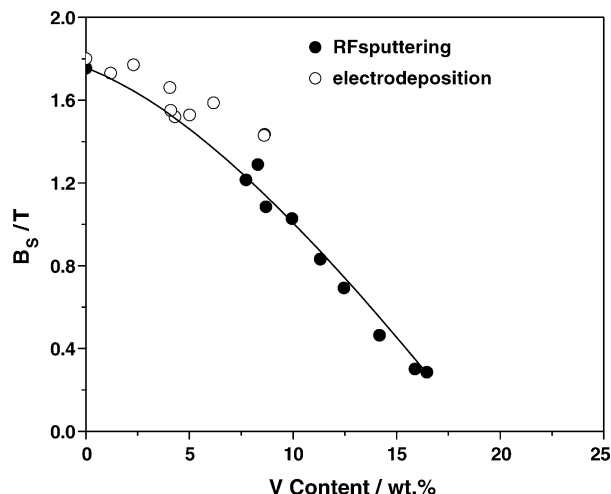


Fig. 8. Comparison of magnetic saturation of Co-V alloys by electrodeposition and sputtering at various V deposit contents.

Fig. 8 compares magnetic saturation of electrodeposited Co-V with RF sputtered Co-V deposits as a function of deposit V content [27]. Both exhibit decreasing magnetic saturation with increasing deposit V content.

3.2. Fe-V Electrodeposits

Fig. 9 shows the effects of increasing CD and pH on deposit composition. The Fe deposit content increases linearly; conjointly the deposit V content decreases (Fig. 9a). Increasing solution pH (CD = 3 mA cm⁻²), however, shows a converging, practically linear trend (Fig. 9b).

Decreasing deposit V content with increasing applied CDs can be explained by the resulting variations in the partial CDs. As shown in Table 5, when the applied CD is increased (pH = 6.0), the partial CDs of V and Fe increased with the increasing rate for Fe greater than for V; thus, the V content decreases with increasing CD (Fig. 9a). Similarly, when solution pH is increased (CD = 3 mA cm⁻²), the partial CD of V deposition remains almost constant, whereas the partial CD

Table 5
Partial current density and current efficiency of Fe-V electrodeposits

	i_V (mA/cm ²)	i_{Fe} (mA/cm ²)	I_{H_2} (mA/cm ²)	CE (%)
i_{total} (mA/cm ²) ^a				
3	0.02	0.41	2.57	14
5	0.03	0.85	4.12	18
10	0.04	1.84	8.12	19
25	0.11	4.14	20.75	17
50	0.11	7.78	42.11	16
pH ^b				
5.5	0.02	0.50	2.48	17
6.0	0.02	0.41	2.57	14
6.5	0.02	0.35	2.63	12
7.0	0.01	0.29	2.70	10

^a pH 6.0.

^b CD: 3 mA/cm².

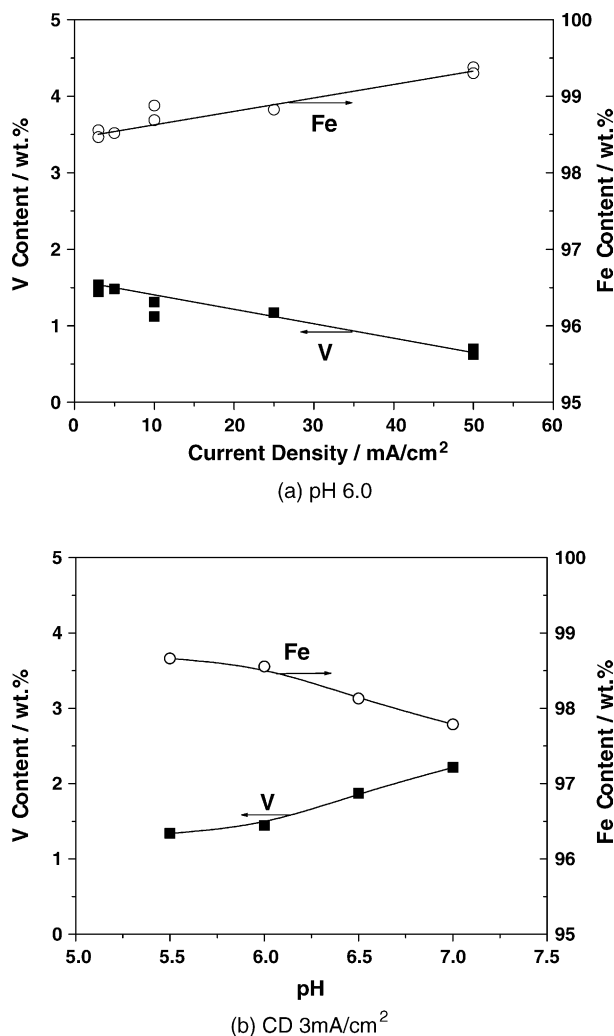


Fig. 9. Composition of Fe-V electrodeposits obtained at various current densities (a) and solution pH (b).

of Fe decreased (Table 5), resulting in increased deposit V contents (Fig. 9b).

The CEs of deposits from pH = 6.0 solutions do not change appreciably (14–19%) with the applied CD (Table 5). Increasing solution pH (CD = 3 mA cm⁻²) results in decreased CEs, however (Table 5).

Fig. 10 shows structural changes of Fe-V electrodeposits as a result of solution pH. The XRD spectra of Fe-V alloys deposited at pH 6.0 and 7.0 are compared with Fe deposited at the same experimental conditions. The bcc (110) plane was the preferred orientation for both Fe-V and Fe electrodeposits. However, Fe-V deposits exhibit two additional planes, bcc (200) and bcc (211), with weaker intensities. The addition of V to the Fe matrix is likely the main factor for the development of the bcc (200) and (211) planes. The intensity of the planes decreased slightly in deposits from increased solution temperature (50 °C) (Fig. 5b). Magnetic saturation of deposits from 25 °C solution was 2.05 T; this decreased substantially for the dark, non-metallic deposits from 50 °C solutions, because of oxide/hydroxide inclusions. In-

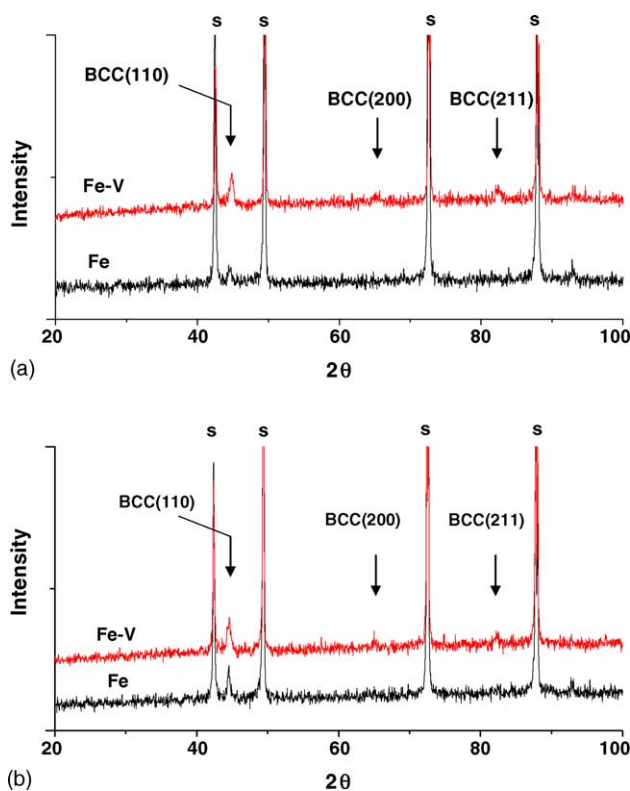


Fig. 10. XRD results of Fe-V and Fe electrodeposits at pH 6.0 and 7.0; CD = 3 mA/cm²: (a) Fe-V (1.5 wt.% V) and Fe at pH 6.0; (b) Fe-V (2.2 wt.% V) and Fe at pH 7.0.

creased solution temperature (75 °C) resulted in instability of the solution with precipitation of Fe(OH)₂, possibly because of insufficient citrate concentration.

Nevitt and Aldred [28] calculated the magnetic saturation of electrodeposited Fe (2.15 T) and Fe-V electrodeposited alloys, the latter decreasing almost linearly with increasing V content. Table 6 shows the experimental values for magnetic saturation (B_s) of Fe-V electrodeposits from 0.7 to 1.5 wt.% V (solution pH = 6) are in reasonable agreement with the calculated values. Deposits containing 1.9 and 2.2 wt.% vanadium deviated from the calculated values. The differences might be the result of different deposition conditions; the latter deposits were electrodeposited at pH 6.5 and pH 7.0, respectively. At the higher solution pH's, the deposits prob-

Table 6
Effect of vanadium content on the magnetic saturation of Fe-V electrodeposits

V content (wt.%)	B_s [28] (T)	B_s (experimental) (T)	pH
0.7	2.13	2.21	6.0
1.1	2.12	2.00	6.0
1.3	2.11	2.13	5.5
1.4	2.11	2.05	6.0
1.4	2.11	2.13	6.0
1.5	2.11	2.05	6.0
1.9	2.10	1.88	6.5
2.2	2.09	1.93	7.0

CD = 3 mA/cm²; deposit thickness = 1.2 μm.

Table 7
Effect of pH and CD on deposit composition and coercivity of Ni–V electrodeposits

	Ni (wt.%)	V (wt.%)	CE (%)	$H_c //$ (Oe)	$H_c \perp$ (Oe)
pH ^a					
5.5	99.65	0.35	14.3	94	76
6.0	99.27	0.73	13.5	102	69
6.5	99.63	0.37	10.9	110	105
7.0	99.56	0.44	11.5	128	133
CD (mA/cm ²) ^b					
3	99.27	0.73	13.5	102	69
5	99.15	0.85	13.7	98.4	90.8
10	99.37	0.63	10.2	93.4	73.7
50	99.79	0.21	14.2	115	141

^a CD = 3 mA/cm².

^b pH = 6.0.

ably contained oxide and/or hydroxide contaminants which reduce magnetic saturation.

The coercivity (H_c) of Fe–V electrodeposits (V contents 0.5–2.25 wt.%) deposited from solutions with pH between 5.5 and 7.0 was measured in the parallel and perpendicular directions. In the parallel direction, the coercivity ($H_c = 27$ Oe) was independent of the deposit V content. In the perpendicular direction, the coercivity increased with increasing deposit V content.

Comparison of the magnetic properties of electrodeposited Fe and Fe–1.5V alloy (Table 4) indicates slightly higher magnetic saturation (B_s) for Fe (2.10 T) than Fe–V alloy (2.05 T). The coercivity of the Fe deposit (94 Oe) was higher than the Fe–V deposit (27 Oe).

3.3. Ni–V electrodeposits

Because electrodeposited Ni has lower magnetic saturation (0.6 T) than either Co or Fe, a limited exploratory investigation of electrodeposited Ni–V alloys is presented. Ni–V deposit compositions and properties as a result of varying solution pH and CD are shown in Table 7. Under the deposition conditions investigated, the deposit V content was less than 1 wt.%. The current efficiencies ranged between 10 and 14%. The coercivities of the deposits did not vary greatly as a result of the minor variations in deposit composition.

The Ni–V electrodeposits show preferred fcc (1 1 1), fcc (2 0 0) and fcc (2 2 0) planes, the peak intensities increasing in deposits from increased solution temperatures (Fig. 5c); the deposit V contents decreased (CD = 3 mA cm⁻², pH = 6.0). Increasing peak intensities with deposition from increased solution temperatures are indicative of increased GS.

4. Conclusions

Increased deposit V content was obtained by addition of NH₃ (aq.) in the aqueous electrodeposition of binary iron group–vanadium alloys from citrate solutions. Deposit V content increased with increasing solution pH; however, de-

posits from solution pH > 7 were non-metallic. Increasing current density resulted in a decrease in vanadium content and a sharp increase in H₂ evolution (decreased current efficiency).

For Co–V (≥ 4.3 wt.% V), the preferred orientation changes from HCP (0 0 2) to HCP (1 0 0). This change in orientation possibly contributes to the deposit magnetic properties; e.g., Co–V deposits with (1 0 0) planes exhibit harder magnetization (higher coercivities) than deposits with (0 0 2) planes. The GS of deposits containing ≈ 4 wt.% vanadium did not vary substantially (12–16 nm). Deposits with higher vanadium content exhibited GS ~ 41 nm for (1 0 0) planes and 14 nm for (1 1 0) planes. Both electrodeposited and sputtered Co–V deposits exhibit decreased magnetic saturation with increasing deposit V content.

The Fe–V deposit compositions show similar trends as Co–V deposits. However, substantially less vanadium (≈ 2 wt.%) is incorporated into the deposits. The bcc (1 1 0) preferred orientation of Fe–V deposits is similar to that of electrodeposited Fe but with two additional phases, bcc (2 0 0) and (2 1 1) planes, present.

Magnetic saturation of Fe–V deposits decreases with increased deposit V content. Deposit coercivities increase in the perpendicular direction, with increasing vanadium content; however, coercivities do not change significantly in the parallel direction.

Nickel vanadium deposits contained <1 wt.% V under similar solution pH and current density ranges. In general, the amount of V co-deposited increased as follows: Ni < Fe \ll Co.

Acknowledgment

This work was supported by the DARPA MEMS program (DABT 63-99-1-0020) and the NSF xyz on a chip program.

References

- [1] A. Brenner, *Electrodeposition of Alloys*, vol. II, Academic Press, 1963, p. 239.
- [2] S.N. Srimathi, S.M. Mayanna, B.S. Sheshadri, *Surf. Technol.* 16 (1982) 277.
- [3] I.W. Wolf, *J. Electrochem. Soc.* 108 (1961) 959.
- [4] H.V. Venkatesetty, *J. Electrochem. Soc.* 117 (1970) 403.
- [5] L.T. Romankiw, P. Simon, *IEEE Trans. Mag. Mag.* 11 (1) (1975) 50.
- [6] P.C. Andricacos, L.T. Romankiw, in: H., Gerischer, C.W., Tobias, (Eds.), *Adv. Electrochem. Sci. & Engr.*, vol. 3, VCH, New York, 1994, p. 227.
- [7] D. Gangasingh, J.B. Talbot, *J. Electrochem. Soc.* 138 (1991) 3605.
- [8] W.C. Grande, J.B. Talbot, *J. Electrochem. Soc.* 140 (1993) 669.
- [9] K.Y. Sasaki, J.B. Talbot, *J. Electrochem. Soc.* 145 (1998) 981.
- [10] H. Dahms, I.M. Croll, *J. Electrochem. Soc.* 112 (1965) 771.
- [11] S. Hessemer, C.W. Tobias, *J. Electrochem. Soc.* 136 (1989) 3611.
- [12] W.C. Grande, J.B. Talbot, *J. Electrochem. Soc.* 140 (1993) 675.
- [13] K.Y. Sasaki, J.B. Talbot, *J. Electrochem. Soc.* 147 (2000) 189.

- [14] M. Matlosz, *J. Electrochem. Soc.* 140 (1993) 2272.
- [15] D.L. Grimmett, M. Schwartz, K. Nobe, *J. Electrochem. Soc.* 137 (1990) 3414.
- [16] N.H. Phan, M. Schwartz, K. Nobe, *J. Appl. Electrochem.* 21 (1991) 672.
- [17] S.H. Liao, *IEEE Trans. Mag.* 23 (1987) 2981.
- [18] S.H. Liao, *IEEE Trans. Mag.* 26 (1990) 328.
- [19] S.H. Liao, US Patent 5,168,410 (1992).
- [20] J.W. Chang, P.C. Andricacos, B. Petek, L.T. Romankiw, *Proc. ECS* 92 (10) (1992) 275.
- [21] (a) P.J. Partain, M.B. Balmas, M. Schwartz, K. Nobe, *Proc. 80th AESF Annu. Tech. Conf.* (1993) 707;
(b) C. Arcos, M. Schwartz, K. Nobe, *Proc. ECS* 95 (18) (1995) 63;
(c) M. Schwartz, C. Arcos, K. Nobe, *Plat. Surf. Fin.* 90 (6) (2003) 46.
- [22] G.Y. Chin, J.H. Wernick, in: E.P. Wohlfarth (Ed.), *Ferromagnetic Materials*, vol. 2, North-Holland, 1980 (Chapter 2).
- [23] C.-W. Chen, *Magnetism and Metallurgy of Soft Magnetic Materials*, Dover, 1986, p. 390.
- [24] C.K. Gupta, N. Krishnamurthy, *Extractive Metallurgy of Vanadium*, Elsevier, 1992, p. 122.
- [25] A.J. Bard (Ed.), *Encyclopedia of Electrochemistry of the Elements*, vol. VII, 1976, p. 394.
- [26] S. Armyanov, *Electrochim. Acta* 45 (2000) 3323.
- [27] K. Fukuda, Y. Kitahara, F. Maruta, J. Ezaki, *IEEE Trans. Mag.* 18 (1982) 1116.
- [28] M.V. Nevitt, A.T. Aldred, *J. Appl. Phys.* 34 (1963) 463.